Comparsion and Analysis of Heat Transfer in a Porous Aluminum Foam Using Local Thermal Equilibrium and Local Thermal Non-equilibrium Models

Lin, Wamei; Xie, Gongnan; Yuan, Jinliang; Sundén, Bengt

2013

IWHT2013-067

Comparison and analysis of heat transfer in a porous aluminum foam using local thermal equilibrium and local thermal non-equilibrium models

W.M. Lin[a], G.N. Xie[b], J.L. Yuan[a], B. Sundén[a]*

[a]Department of Energy Sciences, Lund University, P.O.Box 118, Lund, 22100, Sweden
[b]School of Mechanical Engineering, Northwestern Polytechnical University, P.O. Box 552, Xi'an, Shaanxi 710072, China

(*Corresponding author: bengt.sunden@energy.lth.se)

Abstract

Aluminum foams are favorable in modern thermal engineering applications because of the high thermal conductivity and the large specific surface area. The present study is to investigate an application of a porous aluminum foam by using local thermal equilibrium (LTE) and local thermal non-equilibrium (LTNE) heat transfer models. Three-dimensional simulations of laminar flow (for porous foam zone), turbulent flow (for open zone) and heat transfer are performed by a computational fluid dynamics (CFD) approach. Meanwhile, the Forchheimer extended Darcy's law is employed for evaluating the fluid characteristics. The simulation results are compared with the experimental data in the literature. By comparing and analyzing the local and average Nusselt number, it is found that the LTNE and LTE models can obtain the same Nusselt numbers inside the aluminum foam when the air velocity is high, meaning that the aluminum foam is in a thermal equilibrium state. Besides that, a low interfacial heat transfer coefficient is required for the aluminum foam to reach a thermal equilibrium state as the height of the aluminum foam is increased. This study suggests that the LTE model could be applied to predict the thermal performance for the high fluid velocity case or for the case with large height.

Keywords: Porous aluminum foam, Local thermal non-equilibrium (LTNE), Local thermal equilibrium (LTE), Heat transfer, Simulation, CFD

1 Introduction

Due to the large specific surface area, the porous structure of aluminum foams can enlarge the surface for heat transfer. Meanwhile, the irregular structure induces a tortuous flow and breaks the thermal boundary to produce high thermal performance. Thus, the porous aluminum foams are favorable in modern thermal engineering applications, such as electronic cooling, thermal energy absorber, and so on.

There are two major simulation models to analyze the thermal performance of porous media: (1) local thermal equilibrium (LTE) model, in which the fluid phase and solid phase are assumed to be at the same temperature. The effective thermal conductivity (λ_{eff}) of the porous media is used to consider effect of the fluid and solid thermal conductivity. Due to the effect of the curly thermal path (thermal tortuosity) and the different structures of the porous materials, there are many different formulas for λ_{eff} based on the experimental work or theoretical analysis [1-6]. (2) local thermal non-equilibrium (LTNE) model, in which there is a temperature difference between the fluid phase and the solid phase, an interfacial heat transfer coefficient (h_{sf}) has to be specified to connect the thermal energy transport between the solid part and the fluid part. There exist various equations to evaluate the h_{sf} in different porous structures [7-9].

A temperature difference between the solid phase and the fluid phase was assumed because of the large difference of the thermal conductivity between the solid phase and fluid phase inside the aluminum foam. This is the main reason why there are many research works of the metal foam using the LTNE model to analyze the heat transfer inside aluminum foams. For example, Aniri et al. [10] presented the validity of LTE condition, and drew the comprehensive error maps of LTE based on the numerical results. Lee et al. [11] also investigated the validity of LTE model, and presented a conceptual assessment of solid and fluid temperature differentials. The error by using the LTE model was increased when the difference of thermal conductivity between solid phase and fluid phase was increased. Meanwhile, Calmidi et al. [7] used experimental and numerical methods to quantify the thermal non-equilibrium effects in metal foams. Other research works concerning metal foams based on the LTNE model can be found in [12-15].

Furthermore, Mahjoob et al. [16] and Alazmi et al. [17] presented a comprehensive literature review of fluid and thermal transport models within porous media.

However, when the fluid velocity is very high, the metal foam and the fluid could be in a near "thermal equilibrium" state, due to the high interfacial heat transfer coefficient and the large specific surface area. According to [9], it was found that when the air mean velocity was larger than 3 m/s, the solid and fluid were in near thermal equilibrium but a large error occured in the extracted heat transfer coefficient results compared with experimental results. On the other hand, Kim et al. [18] obtained the analytical solutions of temperature distribution in the microchannel heat sink (whose fluid and thermal characteristics were similar to those in the porous media) by using both LTE and LTNE model. It was shown that the LTE model could be practically used in microchannel heat sinks with high porosity. Jeng et al. [19] applied the fin theory and the concept of thermal network to estimate the heat transfer of the porous sink. Based on the results, the phase in local thermal equilibrium could occur at a large height of the porous heat sink and high Reynolds number.

Based on a literature review, the LTNE model is found to be more complicated than the LTE model in solving two equations and defining more parameters (interfacial heat transfer coefficient (hsf) and specific surface area (asf)). However, the simple LTE model can estimate as accurately as the LTNE model in some thermal applications. In order to explore deeply in what engineering applications the LTE model can be used, instead of using the LTNE model, the present study aims to investigate the thermal performance of a porous aluminum foam by using the LTE and LTNE heat transfer models. Meanwhile, the Forchheimer extended Darcy's law is employed to analyze the fluid characteristics. The Nusselt numbers calculated by the LTNE and LTE model are compared. It is found that the LTE model can predict the thermal performance of the aluminum foam as accurately as the LTNE model at high air velocity.

Nomenclature

a	= specific surface area (m^{-1})
A	= area (m^2)
c_p	= specific heat (J/kgK)
C_F	= Forchheimer coefficient
D	= diameter (m)
h	= heat transfer coefficient (W/m^{2}K)
H	= height (m)
k	= turbulent kinetic energy (m^2/s^2)
L	= length (m)
Nu	= Nusselt number
p	= pressure (Pa)
Pr	= Prandtl number
PPI	= pores per inch
q	= heat flux (W/m^2)
Q	= disspated heat (W)
T	= temperature (K)
u, v, w	= velocity components in x, y and z directions (m/s)
$u_i^{'}$	= fluctuation from the mean velocity u_i (m/s)
W	= width (m)
Δp	= pressure drop (Pa)
$\triangle T$	= temperature difference (K)

$\overline{T}$	= average temperature (K)

Greek Symbols

α	= permeability (m^2)
ε	= rate of energy dissipation
λ	= thermal conductivity (W/mK)
μ	= dynamic viscosity (Pas)
ρ	= density (kg/m^3)
τ	= tortuosity
φ	= porosity

Subscripts

b	= base
eff, e	= effective
f	= fluid
h	= hydraulic
in	= inlet
i, j	= coordinate indices
out	= outlet
p	= pore
s	= solid
t	= turbulence
w	= wall

2 Physical model

A simplified configuration of the porous aluminum foam is shown in Fig. 1. The aluminum foam with uniform porosity is placed in a rectangular channel, and the foam is heated from its top and bottom surface symmetrically. Thus, only half height of the channel is analyzed in this study. The overall size of the core of the aluminum foam is: 15.24 cm × 5.08 cm × 15.24 cm (W×H×L). The fluid is assumed to be incompressible with constant properties, and the flow is at steady-state. The parameters of the porous aluminum foam are listed in Table 1.
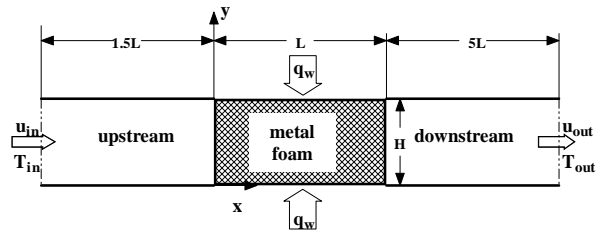

Fig. 1. Schematic of a 2D model configuration for the porous foam

Table 1. The properties of the studied aluminum foam [9]

Foam sample	α (m^2)	C_F	φ	D_p (m)	λ_{se} (W/m K)	a (m^{-1})
40 PPI	6.98 ×10^{-9}	0.02	0.918	5.08 ×10^{-4}	9.78	2760

3 Mathematical formulation and numerical method

3.1 Computational domain

In order to make sure the aluminum foam is located in the fully developed flow region, the computational domain is extended upstream 1.5 times the aluminum foam sample length to eliminate the entrance length effect. Similarly, the computational domain is extended downstream 5 times the length of the aluminum foam sample to achieve the one-way coordinate assumption at the domain outlet. Thus, the whole stream length of the computational domain is 7.5 times the actual aluminum foam length, as shown in Fig. 1.

3.2 Adoption of flow model

In this study, the air inlet velocity of the upstream channel is ranging from 0.7 to 5 m/s with the corresponding Reynolds number on the air side is ranging from 3387 to 24190. Thus, low Reynolds number turbulent flow prevails in the channel. However, laminar flow prevails inside the aluminum foam. This might be so, because it is difficult to generate turbulent eddies in the small open cells of the aluminum foam. In order to capture the low Reynolds number characteristics in the turbulent flow, the "renormalization group" (RNG) k-ε turbulence model is adopted [20-21] on the air side. Furthermore, due to the laminar flow inside the aluminum foam, the RNG k-ε turbulence model might be useful to take into account the low - Reynolds number effect near the foam walls.

3.3 Mathematical formulation

According to the above presented assumptions, the governing equations for continuity, momentum and thermal energy may be expressed as follows:

3.2.1 Air zone governing equations (turbulent flow)

Continuity equation

$$\frac{\partial\left(\rho_f u_i\right)}{\partial x_i} = 0 \tag{1}$$

Momentum equations

$$\frac{\partial\left(\rho_f u_i u_j\right)}{\partial x_j} = -\frac{\partial p}{\partial x_i} + \frac{\partial}{\partial x_j}\left(\left(\mu_f + \mu_t\right)\left(\frac{\partial u_i}{\partial x_j} + \frac{\partial u_j}{\partial x_i}\right)\right) \tag{2}$$

Energy equation

$$\frac{\partial\left(\rho_f u_j T\right)}{\partial x_j} = \frac{\partial}{\partial x_j}\left(\left(\frac{\mu_f}{\Pr_f} + \frac{\mu_t}{\Pr_t}\right)\frac{\partial T}{\partial x_j}\right) \tag{3}$$

The equations of the turbulent kinetic energy k and the rate of energy dissipation ε corresponding to the RNG k-ε turbulence model are as follows.

Turbulent kinetic energy k equation:

$$u_j \frac{\partial k}{\partial x_j} = -\overline{u_i' u_j'}\frac{\partial u_i}{\partial x_j} + \frac{\partial}{\partial x_j}\left(\frac{K_m}{\sigma_k}\frac{\partial k}{\partial x_j}\right) - \varepsilon \tag{4}$$

Rate of energy dissipation ε equation:

$$u_j \frac{\partial \varepsilon}{\partial x_j} = -C_{\varepsilon 1}\frac{\varepsilon}{k}\overline{u_i' u_j'}\frac{\partial u_i}{\partial x_j} + \frac{\partial}{\partial x_j}\left(\frac{K_m}{\sigma_\varepsilon}\frac{\partial \varepsilon}{\partial x_j}\right) - C_{\varepsilon 2}\frac{\varepsilon^2}{k} - R \tag{5}$$

where, $R = \dfrac{C_\mu \eta^3 \left(1 - \eta \eta_0\right)\varepsilon^2}{\left(1 + \beta_0 \eta^3\right)k}$, $\quad \mu_t = \rho C_\mu \dfrac{k^2}{\varepsilon}$,

$$\eta = \frac{k}{\varepsilon}\left[\left(\frac{\partial u_i}{\partial x_j} + \frac{\partial u_j}{\partial x_i}\right)\frac{\partial u_i}{\partial x_j}\right]^{0.5},$$

$$K_m = v\left[1 + \left(\frac{C_\mu}{v}\right)^{0.5}\frac{k}{\varepsilon^{0.5}}\right]^2,$$

and v is the kinematic viscosity of air; u_i' are the fluctuations of the time-averaged velocity u_i.

The values of the constants are as follows:
$C_\mu = 0.0845; \sigma_k = 0.7179; \sigma_\varepsilon = 0.7179;$
$C_{\varepsilon 1} = 1.42; C_{\varepsilon 2} = 1.68; \beta_0 = 0.012; \eta_0 = 4.377.$

3.2.2 Aluminum foam zone governing equations (laminar flow)

Because the aluminum foam is a porous medium, the Forchheimer extended Darcy's law has been applied for the air pressure drop through the aluminum foam. Due to the porous structure, the thermal length inside the aluminum foam has to be modified by the tortousity of the foam, which is the ratio of the actual flow path length average (L_e) to the length (L) of the porous medium in the direction of the macroscopic flow, $\tau = L_e / L$ [22]. On the other hand, because the effective thermal conductivity of the porous foam is dominated by the thermal conductivity of aluminum, the thermal dispersion is ignored in the energy equation. Thus, the governing equations for the graphite foam are as follows:

Continuity equation:

$$\frac{\partial\left(\rho_f u_i\right)}{\partial x_i.\varphi} = 0 \tag{6}$$

Momentum equations:

$$\frac{\partial\left(\rho_f u_i u_j\right)}{\partial x_j} = -\varphi\frac{\partial p}{\partial x_i} + \frac{\partial}{\partial x_j}\left(\mu_f\left(\frac{\partial u_i}{\partial x_j} + \frac{\partial u_j}{\partial x_i}\right)\right)$$
$$-\varphi\left(\frac{\mu_f}{\alpha}u_i + \frac{\rho_f C_F}{\sqrt{\alpha}}|u|u_i\right) \tag{7}$$

Energy equation:
   a.   LTE case

$$\varphi\frac{\partial\left(\rho_f c_{p.f} u_j T\right)}{\partial x_j} = \lambda_{eff}\frac{\partial}{\partial x_j}\left(\frac{\partial T}{\partial x_j}\right) \tag{8}$$

   b.   LTNE case

for fluid:

$$\varphi\frac{\partial\left(\rho_f c_{p.f} u_j T_f\right)}{\partial x_j} = \lambda_{fe}\frac{\partial}{\partial x_j}\left(\frac{\partial T_f}{\partial x_j}\right) + h_{sf}a_{sf}\left(T_s - T_f\right) \tag{9}$$

for solid:

$$0 = \lambda_{se}\frac{\partial}{\partial x_j}\left(\frac{\partial T_s}{\partial x_j}\right) - h_{sf}a_{sf}\left(T_s - T_f\right) \tag{10}$$

where, $\lambda_{fe} = \lambda_f \varphi / \tau, \lambda_{se} = \lambda_s (1-\varphi) / \tau, \lambda_{eff} = \lambda_{fe} + \lambda_{se}$[14].

The value of τ, h_{sf} and a_{sf} are adopted from the experimental work in [9]. φ is the porosity of the porous aluminum foam; α the permeability of the porous aluminum foam (m^2); C_F the Forchheimer coefficient.

3.4 Boundary conditions

The momentum and energy transports are calculated simultaneously for the air and porous aluminum foam zones. The boundaries on the aluminum foam left- and right walls are set up as "interior surfaces" or interfaces. Thus, the solutions for the momentum and energy transports on the interfaces between upstream/downstream air and porous aluminum foam zones are not required. The necessary boundary conditions are as follows:

(1) For the upstream extended region (-1.5L≤x＜0)
At the inlet (x=-1.5L):
$u = const$, $T = const$, $v = w = 0$
At the upper and lower boundaries (y=0, y=H):
$$\frac{\partial u}{\partial y} = \frac{\partial w}{\partial y} = 0, \quad v = 0, \quad \frac{\partial T}{\partial y} = 0$$
At the sides of z=0 and z=W:
$$\frac{\partial u}{\partial z} = \frac{\partial v}{\partial z} = 0, \quad w = 0, \quad \frac{\partial T}{\partial z} = 0$$

(2) For the downstream extended region (L＜x≤6L)
At the upper and lower boundaries (y=0, y=H):
$$\frac{\partial u}{\partial y} = \frac{\partial w}{\partial y} = 0, \quad v = 0, \quad \frac{\partial T}{\partial y} = 0$$
At the sides of z=0 and z=W:
$$\frac{\partial u}{\partial z} = \frac{\partial v}{\partial z} = 0, \quad w = 0, \quad \frac{\partial T}{\partial z} = 0$$
At the outlet boundary (x=6L):
$$\frac{\partial u}{\partial x} = \frac{\partial v}{\partial x} = \frac{\partial w}{\partial x} = \frac{\partial T}{\partial x} = 0$$

(3) For the aluminum foam region (0≤x≤L)
At the sides of z=0 and z=W:
$$\frac{\partial u}{\partial z} = \frac{\partial v}{\partial z} = 0, \quad w = 0, \quad \frac{\partial T}{\partial z} = 0$$
At the upper boundary (y=H):
$$\frac{\partial u}{\partial y} = \frac{\partial w}{\partial y} = 0, \quad v = 0, \quad \frac{\partial T}{\partial y} = 0$$
At the lower boundaries (y=0):
$u = v = w = 0$, $q_w = const$

3.5 Numerical method and grid independence test

The commercial code ANSYS FLUENT 14.0 is used for the numerical solution. A control-volume-based technique is adopted to convert the governing equations to algebraic equations so that these can be solved numerically [23]. The Semi-Implicit Method for Pressure Linked Equations (SIMPLE) algorithm is used to couple the pressure and velocity. A second-order upwind scheme is used for the space discretization of the momentum, energy and turbulence equations in the simulations.

A second-order scheme is applied to the space discretization of pressure as well. The residual of the continuity, components of velocity, k and ε is set to be below 10^{-3}, while for energy it is below 10^{-6}.

A hexagonal mesh is generated by using the blocking technique in the ICEM software, as shown in Fig. 2. In order to control the grid independence, three sets of mesh size (Mesh I: 80×20×60; Mesh II: 120×30×80; Mesh III: 200×50×120 (W×H×L)) were selected for the aluminum foam region to find out the grid dependence. It is found that the deviation of pressure drop is between 0.07 - 0.35%, and the deviation of Nusselt number is between 0.12 - 0.65 %, as shown in Table 2. Based on this, a mesh size of 120×30×80 was adopted in the simulation.
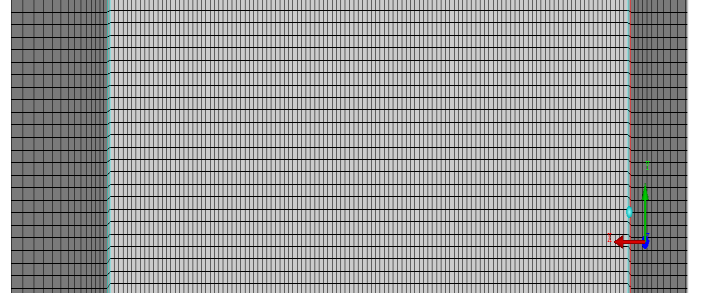

Fig. 2. Typical hexagonal mesh for the computations.

Table 2. Grid independence test (u=1.2m/s)

	Mesh I	Mesh II	Mesh III
	80×20×60,	120×30×80	120×30×80
Δp (Pa)	1427	1433	1432
Nu	3413	3387	3391
|Δp| deviation	0.35 %	0.07%	base line
|Nu| deviation	0.65 %	0.12%	base line

3.6 Evaluation of performance parameters

In order to compare the thermal performance difference between LTE and LTNE models, the average Nusselt number (Nu) for the solid wall (y = 0) is defined to characterize the thermal performance of the aluminum foam.

$$Nu = \frac{hD_h}{\lambda_f} = \frac{D_h Q_{removed}}{\lambda_f A_b \Delta T} = \frac{D_h q_w}{\lambda_f \Delta T} = \frac{D_h q_w}{\lambda_f (\overline{T_w} - (\overline{T_{in}} + \overline{T_{out}})/2)} \quad (11)$$

Where D is the length scale based on either the equivalent particle diameter of the foam or the hydraulic diameter of the channel. A is the area of the effective heat transfer surface or the heated base area of the foam. In this study, D is defined as the hydraulic diameter of the channel D_h, A the heated base area A_b, and ΔT is the mean temperature difference between the heated base temperature and the fluid mean temperature.

Another important parameter is the local Nusselt number (Nu$_x$), which is defined as:

$$Nu_x = \frac{D_h q_w}{\lambda_f (T_{w.x} - \overline{T_x})} \quad (12)$$

4

4. Results and discussion

4.1 Validation of simulation model

Before presenting the simulation results, it is necessary to validate the current simulation model of the aluminum foam. The validation of the LTE model has been presented in [24]. Only the LTNE model will be validated here. The pressure drop (Δp) and the top surface (x = 0.5 H) temperature are calculated and compared with the experimental data [9]. Figure 3 shows the pressure drop of the simulation results and the experimental data. The maximum pressure drop deviation between the simulation and the experimental data are less than 0.9 %. Thus, this simulation model is satisfactory by taking into account the fluid characteristics.

On the other hand, a comparison of the top surface temperature on the porous aluminum foam is shown in Fig. 4. There is a relatively large deviation between the simulation results and the experimental ones at low velocity, i.e., 0.7 m/s. However, the deviation is gradually reduced as the air velocity is increased. Typically quite good agreement between the simulation results and the experimental data is obtained when the air velocity is larger than 1 m/s. Thus, it is believed that the present model is satisfactory and can be applied further to estimate the pressure drop and the thermal performance of the porous aluminum foam.
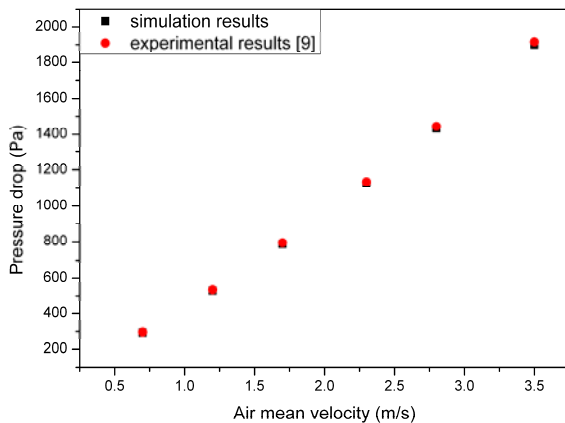

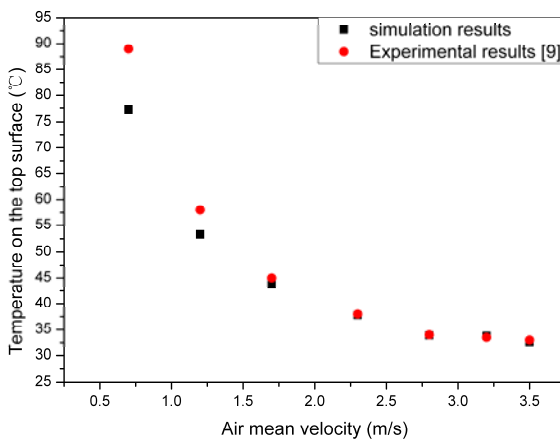**Fig. 3 Pressure drop through the porous aluminum foam (L=0.1524m)**

Fig. 4. The temperature of the top surface (0.5 H) of aluminum foam

4.2 Temperature distribution of aluminum foam

Because the Forchheimer extended Darcy's law has been applied together with the LTE heat transfer model or the LTNE model. This study will only focus on the difference of thermal performance by the LTE and the LTNE model.

Figure 5 shows the air temperature distribution inside the aluminum foam. The maximum temperature in Figs. 5 (a) and (b) is higher than the one in Fig. 5 (c). That is because the air velocity is increased in Fig. 5 (c), and higher air velocity leads to more heat can be dissipated or lower temperature is predicted. On the other hand, when the air velocity is 2.3 m/s, the air temperature near the foam inlet surface (x = 0) is a little bit lower by using the LTE model than the LTNE model. This means that the heat can be dissipated more efficiently by using the LTE model than the LTNE model near the foam inlet surface. In other words, the thermal performance near the foam inlet surface is higher by using LTE model than the LTNE model. However, the temperature distribution becomes similar as the length of the foam is increasing.
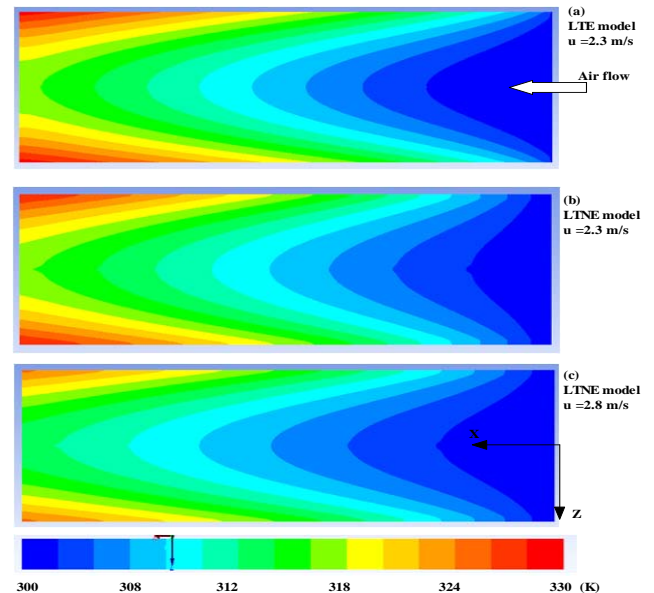

Fig. 5 Air temperature distribution in the aluminum foam

The solid phase and the fluid phase temperature distributions inside the aluminum foam are shown in Fig. 6. By applying the LTNE model, the temperature difference between the solid phase and the fluid phase could easily be seen as the air velocity is 2.3 m/s, as shown in Fig. 6 (a). This means that the aluminum foam is in a local thermal non-equilibrium state when the air velocity is 2.3 m/s. Moreover, due to the thermal resistance in the solid phase is smaller than the one in the fluid phase, the temperature of solid phase is higher than the one of the fluid phase. However, as the air velocity is increased to 4.5 m/s, the temperature distribution in the solid phase becomes as similar as the one in the fluid phase, as shown in Fig. 6 (b). That is mostly because the high air velocity leads to a high interfacial heat transfer coefficient, which can reduce the thermal resistance in the fluid phase. Thus, the temperature difference between the solid phase and the fluid phase is very small. In this case, the aluminum foam is in a near local thermal equilibrium

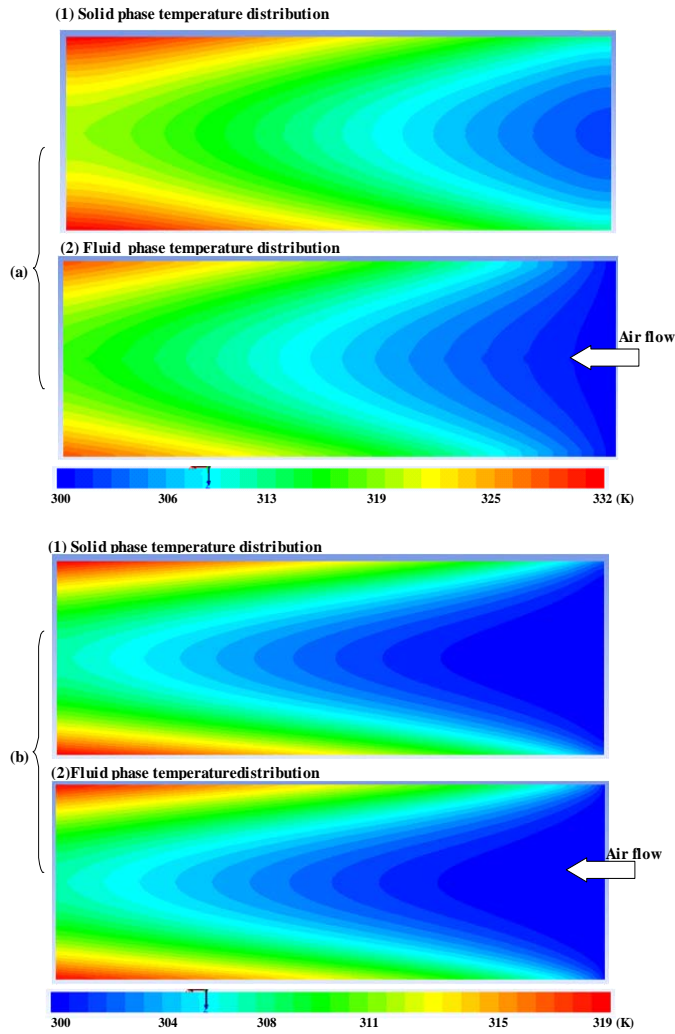state. It is suggested that the LTE model can be applied in the high velocity case.

(1) Solid phase temperature distribution

(2) Fluid phase temperature distribution

(a)

Air flow

| 300 | 306 | 313 | 319 | 325 | 332 (K) |

(1) Solid phase temperature distribution

(b)

(2)Fluid phase temperaturedistribution

Air flow

| 300 | 304 | 308 | 311 | 315 | 319 (K) |

Fig. 6. Solid and fluid temperature distribution inside the aluminum foam by LTNE model: (a) u = 2.3 m/s; (b) u = 4.5 m/s

4.3 Nusselt number by LTNE and LTE model

In order to compare the thermal performance by using the LTNE model and LTE model, the Nusselt number (Nu) is analyzed in this study. Figure 7 shows that the average Nu predicted by both models is increased as the air velocity is increased. When the air velocity is low, the Nu by LTE model is higher than the one by LTNE model at a fixed velocity. This means that the LTE model over-predicts the thermal performance compared to the LTNE model at low velocity. However, the difference in Nu is gradually reduced as the air velocity is increased. When the velocity is larger than 4 m/s, the Nu of the LTE model is similar to that of the LTNE model. This indicates that the aluminum foam has a similar thermal performance by using LTNE and LTE models at high velocity. In other words, the aluminum foam is in a near thermal equilibrium state at high velocities. This is mostly because the high velocity produces high convective effects, and thereby

might lead to a thermal resistance in the fluid phase is of the same order of that in the solid phase. In this sense, the fluid phase and the solid phase could to be at similar temperature distribution when the fluid velocity is high enough.
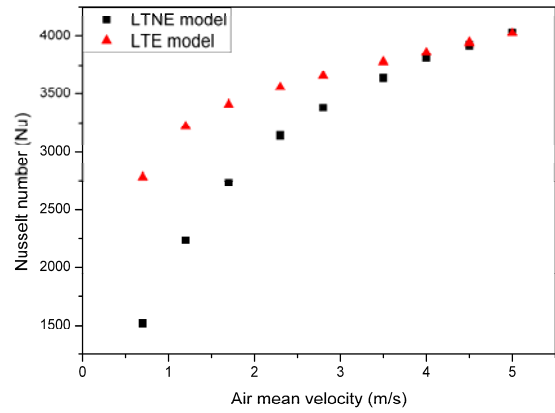

Fig. 7. Average Nusselt number between LTNE and LTE model
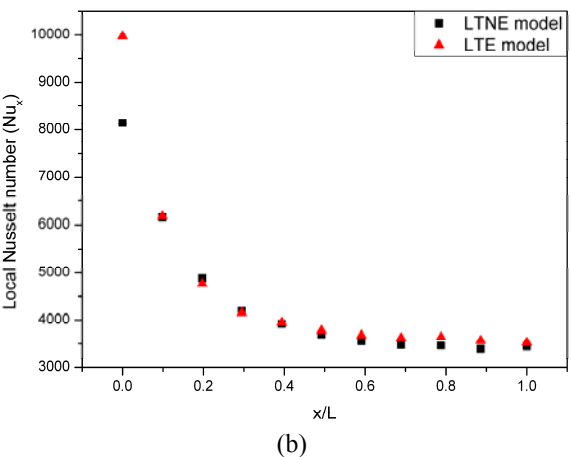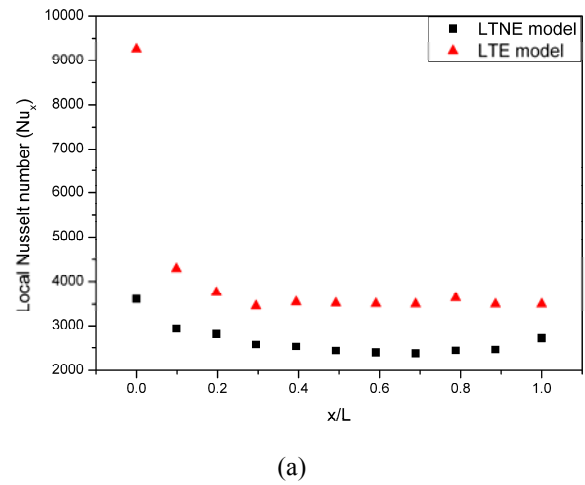

(a)

(b)

Fig. 8. Local Nusselt number along the length under different air velocity: (a) 1.2 m/s; (b) 4 m/s

Figure 8 shows the local Nusselt number (Nu_x) profiles along the bottom length of the aluminum foam. The local Nu_x calculated by the LTE model is higher than the one by the

LTNE model at air velocity of 1.2 m/s, as observed in Fig. 8 (a). This means that the aluminum foam is in a thermal non-equilibrium state along the length with the air in low velocity. However, when the air velocity is increased to 4 m/s, the local Nu_x calculated by the LTE model approaches the one in the LTNE model along the length of the aluminum foam, as shown in Figs. 8 (b). So when the air velocity is high, the aluminum foam is in a "thermal equilibrium" state not only from the overall performance point of view (Fig. 7), but also along the length of the aluminum foam (Fig. 8 (b)).

In addition, Figure 9 shows the effect of different h_{sf} (from 100 to 5000) on the average Nu applied to the aluminum foam. However, the Nu calculated by LTNE model is always around 4000 when the air velocity is 4.5 m/s, implying that the value of h_{sf} does not have much effect on the thermal performance of the aluminum foam when the air velocity is high. From the viewpoint of the LTE model, there is no h_{sf} term in the LTE model (Eq. 8) as the foam is in a thermal equilibrium state. This could explain the reason why Nu would not be changed when the heat transfer coefficient is from 100 to 5000 at air velocity of 4.5 m/s.
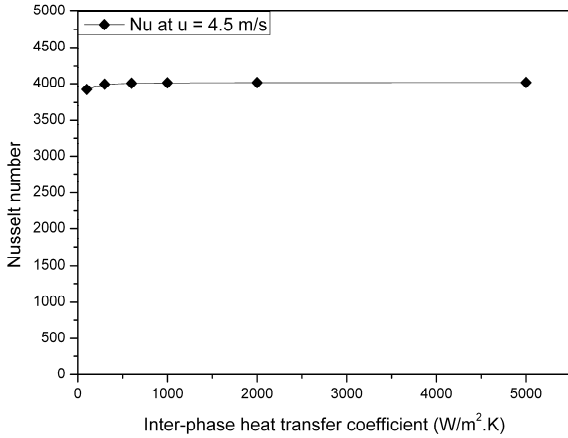

Fig. 9. The effect of heat transfer coefficient on Nu at 4.5 m/s

4.4 Effect of parameters on the LTE state of porous media

The parameters affecting the porous media is whether in a LTNE state or in a LTE state could be λ_{se}, λ_{fs}, H, and φ. When the difference between λ_{se} and λ_{se} is large, a high interfacial heat transfer coefficient h_{sf} is required for the porous media to reach a thermal equilibrium state. On the other hand, if the height (H) of the porous media is reduced, a high value of h_{sf} is required for the porous media to reach a thermal equilibrium state as well. A high h_{sf} needs a high air velocity. As shown in Fig. 10, when the height of the aluminum foam is reduced to 0.5H, the Nu of the LTNE model is closed to the one of LTE model only at a air velocity of around 7 m/s, which is higher than the one in the aluminum foam at the height of 1H (as shown in Fig. 7 around 4 m/s). This is so, as the heat transferring length from the heated base surface becomes shorter as the height of the aluminum foam is reduced. In this case, the thermal resistance in the solid phase is smaller than before. Thus, the thermal resistance in the fluid phase needs to be smaller so as to achieve a thermal equilibrium state. Accordingly, the air velocity has to be increased to reduce the thermal resistance in the fluid phase.
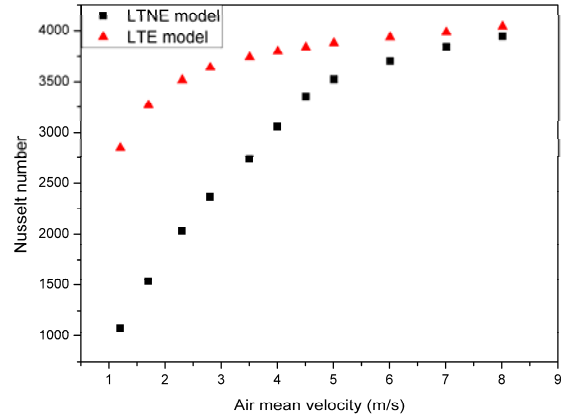

Fig. 10. Nusselt number between LTNE and LTE model (0.5H).

5 Conclusions

The present study investigates the thermal performance of the porous aluminum foam by using the LTE and LTNE models. Three-dimensional flow and heat transfer are studied by a computational fluid dynamics approach. This research aims to discuss probable application of the LTE model and the LTNE model for a specific engineering problem. Through detailed comparisons and analysis, the major conclusions are stated as follows.

(1) By comparing the Nusselt numbers, it is found that the LTE model obtains the same Nusselt numbers inside the aluminum foam as the LTNE model when the air velocity is high. It is suggested that the LTE model is used to predict the thermal performance of aluminum foam at high flow velocities, in which the aluminum foam is considered to be in thermal equilibrium state.

(2) As the aluminum foam is in the thermal equilibrium state, the value of the interfacial heat transfer coefficient does not have any effect on the thermal performance.

(3) When the difference between λ_{se} and λ_{fe} is large or the height of the porous media is reduced, a high flow velocity is required to increase the thermal convection in the porous media to reach thermal equilibrium state.

(4) Even though the LTNE model is very popular in predicting the thermal performance of aluminum foams, the LTE model can be used for high flow velocity cases or if the aluminum foam has a large height.

Acknowledgments

References

[1] Calmidi V. V., Mahajan R. L., The effective thermal conductivity of high porosity fibrous metal foams, ASME Journal of Heat Transfer, 1999, 121:466-471.

[2] Boomsma K., Poulikakos D., On the effective thermal conductivity of a three-dimensionally structured fluid-saturated metal foam, International Journal of Heat and Mass Transfer, 2001, 44:827-836.

7

[3] Bhattacharya A., Calmidi V. V., Mahajan R. L., Thermophysical properties of high porosity metal foams, International Journal of Heat and Mass Transfer, 2002, 45:1017-1031.

[4] Singh R., Kasana H. S., Computational aspects of effective thermal conductivity of highly porous metal foams, Applied Thermal Engineering, 2004, 24:1841-1849.

[5] Yang C., Nakayama A., A synthesis of tortuosity and dispersion in effective thermal conductivity of porous media, International Journal of Heat and Mass Transfer, 2010, 53:3222-3230.

[6] Kuwahara F., Yang C., Ando K., Nakayama A., Exact solutions for a thermal nonequilibrium model of fluid saturated porous media based on an effective porosity, ASME Journal of Heat Transfer, 2011, 133: 112602-(1-9).

[7] Calmidi V. V., Mahajan R. L., Forced convection in high porosity metal foams, ASME Journal of Heat Transfer, 2000, 122:557-565.

[8] Hwang J. J., Hwang G. J., Yeh R. H., Chao C. H., Measurement of interstitial convective heat transfer and frictional drag for flow across metal foams, ASME Journal of Heat Transfer, 2002, 124:120-129.

[9] Garrity P. T., Klausner J. F., Mei R., Performance of aluminum and carbon foams for air side heat transfer augmentation, ASME Journal of Heat Transfer, 2010, 132: 121901-(1-9).

[10] Amiri A., Vafai K., Analysis of dispersion effects and non-thermal equilibrium, non-Darcian, variable porosity incompressible flow through porous media, International Journal of Heat and Mass Transfer, 1994, 37 (6):939-954.

[11] Lee D. Y., Vafai K., Analytical characterization and conceptual assessment of solid and fluid temperature differentials in porous media, International Journal of Heat and Mass Transfer, 1999, 42:423-435.

[12] Lu W., Zhao C. Y., Tassou S. A., Thermal analysis on metal-foam filled heat exchangers. Part I: Metal-foam filled pipes, International Journal of Heat and Mass Transfer, 2006, 49:2751-2761.

[13] Zhao C. Y., Lu W., Tassou S. A., Thermal analysis on metal-foam filled heat exchangers. Part II: Tube heat exchangers, International Journal of Heat and Mass Transfer, 2006, 49:2762-2770.

[14] Xu H. J., Qu Z. G., Tao W. Q., Analytical solution of forced convective heat transfer in tubes partially filled with metallic foam using the two-equation model, International Journal of Heat and Mass Transfer, 2011, 54:3846-3855.

[15] Qu Z. G., Xu H. J., Tao W. Q., Fully developed forced convective heat transfer in an annulus partially filled with metallic foams: An analytical solution, International Journal of Heat and Mass Transfer, 2012, 55:7508-7519.

[16] Mahjoob S., Vafai K., A synthesis of fluid and thermal transport models for metal foam heat exchangers, International Journal of Heat and Mass Transfer, 2008, 51:3701-3711.

[17] Alazmi B., Vafai K., Analysis of variants within the porous media transport models, ASME Journal of Heat Transfer, 2000, 122:303-326.

[18] Kim S. J., Kim D., Lee D. Y., On the local thermal equilibrium in microchannel heat sinks, International Journal of Heat and Mass Transfer, 2000, 43:1735-1748.

[19] Jeng T. M., Tzeng S. C., Hung Y. H., An analytical study of local thermal equilibrium in porous heat sinks using fin theory, International Journal of Heat and Mass Transfer, 2006, 49:1907-1914.

[20] Pope S. B., Turbulent Flows, Cambridge University, 2000.

[21] ANSYS FLUENT 12.0 - Therory Guide, ANSYS, Inc., 2009.

[22] Vallabh R., Banks-Lee P. Seyam A., New approach for determining tortuosity in fibrous porous media, Journal of Engineered Fibers and Fabrics, 2010, 3 (5):7-15.

[23] H. K. Versteeg, W. Malalasekera, An Introduction to Computational Fluid Dynamics, second edition, Pearson Prentice Hall, UK, 2007.

[24] Lin W. M., Sundén B., Yuan J., A performance analysis of porous graphite foam heat exchangers in vehicles, Applied Thermal Engineering, 2013, 50:1201-1210.